A low-cost non-toxic post-growth activation step for CdTe solar cells

ARTICLE *in* NATURE · JUNE 2014

Impact Factor: 42.35 · DOI: 10.1038/nature13435

4 AUTHORS:

Robert Treharne
University of Liverpool
10 PUBLICATIONS **25** CITATIONS
SEE PROFILE

Jonathan D Major
University of Liverpool
27 PUBLICATIONS **111** CITATIONS
SEE PROFILE

Laurie Phillips
University of Liverpool
14 PUBLICATIONS **71** CITATIONS
SEE PROFILE

K. Durose
University of Liverpool
148 PUBLICATIONS **1,367** CITATIONS
SEE PROFILE

LETTER

doi:10.1038/nature13435

A low-cost non-toxic post-growth activation step for CdTe solar cells

J. D. Major[1], R. E. Treharne[1], L. J. Phillips[1] & K. Durose[1]

Cadmium telluride, CdTe, is now firmly established as the basis for the market-leading thin-film solar-cell technology. With laboratory efficiencies approaching 20 per cent[1], the research and development targets for CdTe are to reduce the cost of power generation further to less than half a US dollar per watt (ref. 2) and to minimize the environmental impact. A central part of the manufacturing process involves doping the polycrystalline thin-film CdTe with $CdCl_2$. This acts to form the photovoltaic junction at the CdTe/CdS interface[3,4] and to passivate the grain boundaries[5], making it essential in achieving high device efficiencies. However, although such doping has been almost ubiquitous since the development of this processing route over 25 years ago[6], $CdCl_2$ has two severe disadvantages; it is both expensive (about 30 cents per gram) and a water-soluble source of toxic cadmium ions, presenting a risk to both operators and the environment during manufacture. Here we demonstrate that solar cells prepared using $MgCl_2$, which is non-toxic and costs less than a cent per gram, have efficiencies (around 13%) identical to those of a $CdCl_2$-processed control group. They have similar hole densities in the active layer (9×10^{14} cm^{-3}) and comparable impurity profiles for Cl and O, these elements being important p-type dopants for CdTe thin films. Contrary to expectation, $CdCl_2$-processed and $MgCl_2$-processed solar cells contain similar concentrations of Mg; this is because of Mg out-diffusion from the soda-lime glass substrates and is not disadvantageous to device performance. However, treatment with other low-cost chlorides such as NaCl, KCl and $MnCl_2$ leads to the introduction of electrically active impurities that do compromise device performance. Our results demonstrate that $CdCl_2$ may simply be replaced directly with $MgCl_2$ in the existing fabrication process, thus both minimizing the environmental risk and reducing the cost of CdTe solar-cell production.

The cost of CdTe photovoltaic modules has now dropped below one US dollar per watt and the cost of power generation is rapidly approaching grid parity[2]. A key stage in the fabrication of CdTe solar cells is to anneal the CdTe/CdS p–n structure in the presence of $CdCl_2$. Widely referred to as the 'activation' step, this converts a cell with <2% conversion efficiency to one with typically >10% efficiency and is linked to a number of beneficial structural and electrical changes in both the CdTe and CdS layers[3–6]. $CdCl_2$ contributes to electrical doping, the

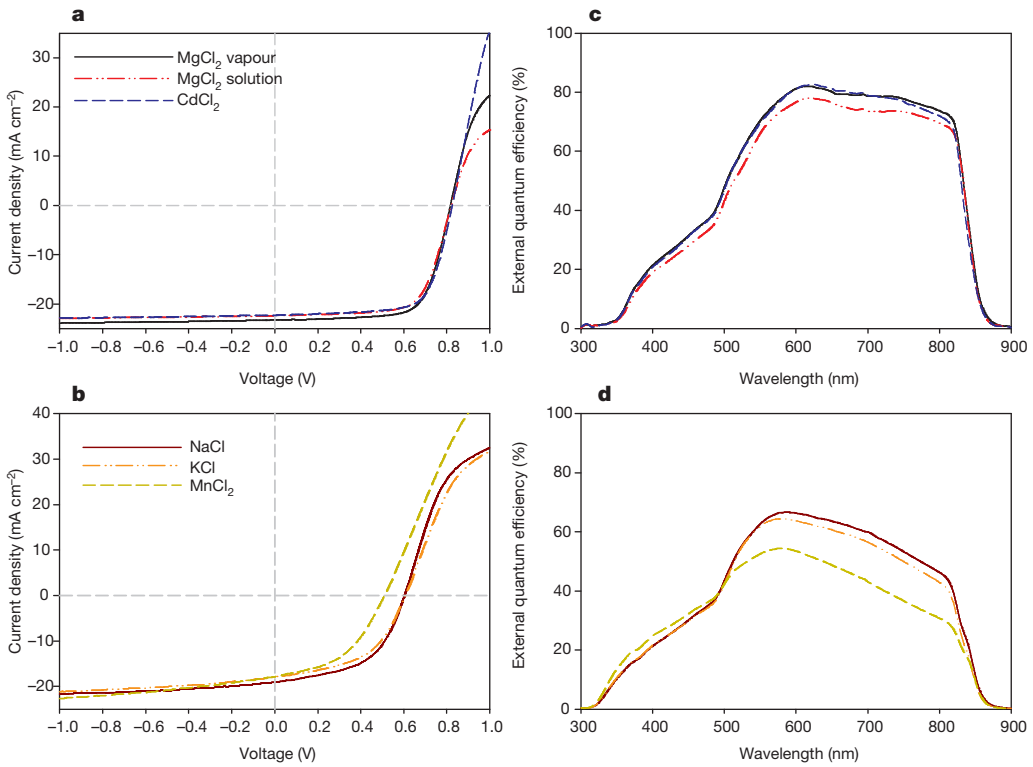

Figure 1 | *J–V* and EQE analysis of cells with different chloride treatments. *J–V* curves for the highest-efficiency contacts for $MgCl_2$-vapour-treated, $MgCl_2$-solution-treated and $CdCl_2$-treated devices (**a**) and for cells activated using the alternative low-cost chlorides, NaCl, KCl and $MnCl_2$ (**b**). All curves show a high degree of 'roll-over' in forward bias. EQE curves for the highest-efficiency contacts for $MgCl_2$-vapour-treated, $MgCl_2$-solution-treated and $CdCl_2$-treated devices (**c**) and for NaCl, KCl and $MnCl_2$ cells that show a decrease in EQE values from short to long wavelength (**d**).

[1]Stephenson Institute for Renewable Energy and Department of Physics, School of Physical Sciences, Chadwick Building, University of Liverpool, Liverpool L69 7ZF, UK.

Table 1 | Peak solar-cell performance for all chlorides tested

Treatment	Peak efficiency (%)	Peak fill factor (%)	Peak J_{sc} (mA cm^{-2})	Peak V_{oc} (V)
$CdCl_2$	13.02	70.01	22.13	0.831
$MgCl_2$ solution	12.71	69.08	22.41	0.821
$MgCl_2$ vapour	13.50	70.24	23.26	0.826
NaCl	6.75	53.34	19.78	0.603
$MnCl_2$	4.37	45.87	18.30	0.520
KCl	5.49	50.11	17.95	0.607

Key solar-cell performance parameters—efficiency η, fill factor, short-circuit current density J_{sc} and open-circuit voltage V_{oc}—for the highest-efficiency contacts for the various activation treatments tested.

recrystallization of small grains and to the passivation of grain boundaries and interface states. The two key drivers in CdTe device research are to limit the environmental impact and to reduce the cost of production. The use of $CdCl_2$ is problematic for both. While CdTe and CdS are both stable, insoluble and are anticipated to contribute little Cd to the environment[7], $CdCl_2$ powder is highly toxic and water soluble, thus posing a risk to both industrial operators and the environment.

$CdCl_2$ also represents a large but inherently avoidable production cost. The bulk cost of $CdCl_2$ is about 0.3 US$ per gram and it requires about 5 tonnes of $CdCl_2$ per gigawatt of solar-cell production, giving an estimated total cost of US$1,500,000 per gigawatt. However, the largest cost associated with $CdCl_2$ processing lies in its handling and disposal, which require a specialized industrial plant for the protection of operators and specialist waste disposal.

However, despite its disadvantages, the use of $CdCl_2$ has endured for more than 25 years[6] and comparatively little effort has been made to identify an effective replacement. A notable exception was the use of the chlorofluorocarbon gas HCF_2Cl (difluorochloromethane)[8], which yielded high-efficiency devices. However, this too posed problems because the gas is linked to ozone depletion and its use has since been restricted by international agreements. Because a viable alternative has never been identified, $CdCl_2$ remains universal in commercial high-efficiency CdTe device production.

Here, we demonstrate that $MgCl_2$ may be used as a direct replacement for $CdCl_2$ in CdTe device manufacturing with no loss in cell performance. $MgCl_2$ has $<1\%$ of the cost per weight (about 0.001 US$ per gram) of $CdCl_2$ and is recoverable from sea water[9]. It is also non-hazardous, environmentally safe and is already used widely—for example, in cold-weather road treatment, as a bath salt and as a food additive in the production of tofu[10]. A process change from $CdCl_2$ to $MgCl_2$ has huge potential instantly to reduce the cost of power generation by CdTe photovoltaics and to minimize the risks in industrial production.

In these experiments, a number of low-cost chlorides ($MgCl_2$, NaCl, KCl and $MnCl_2$) were compared in like-for-like CdTe solar-cell fabrication and performance tests. Other chlorides, which represented either an environmental risk or a high cost (such as $CuCl_2$ and $ZnCl_2$) were not considered. $MgCl_2$ produced the highest efficiencies and was therefore compared more extensively to a standard $CdCl_2$ control process. $MgCl_2$ was applied in two different variations of the basic process, in which the surface of the CdTe is first exposed to the chloride, and then annealed in a tube furnace—see Methods for further details. (1) In the 'solution' process $MgCl_2$ was applied directly to the free CdTe surface in saturated solution in methanol. The samples were then dried to form a layer, and annealed. (2) In the 'vapour' process a glass slide coated with $MgCl_2$ was placed alongside the solar-cell samples directly in the annealing furnace (vapour transport to the CdTe surface occurred during the annealing step itself). Apart from the chloride treatment step, all other device processing was identical.

Current density versus voltage (J–V) curves from the highest-efficiency devices measured under a simulated AM1.5 spectrum are shown in Fig. 1a for the $MgCl_2$ and $CdCl_2$ treatments, with those for other chlorides shown in Fig. 1b. Their external quantum efficiency (EQE) curves are given in Fig. 1c and d, respectively.

The most efficient single device measured (Table 1) was for the $MgCl_2$ vapour treatment. It had an efficiency of 13.50%, a fill factor of 70.24%, a short-circuit current density J_{sc} of 23.36 mA cm^{-2} and an open circuit voltage V_{oc} of 826 mV. The highest efficiency for any $CdCl_2$ control device was 13.02%. However, average performances measured over nine cells (Table 2) showed the $CdCl_2$ and $MgCl_2$-vapour treatments to give identical results within the margin of error, and the $MgCl_2$ solution treatment to yield only slightly reduced efficiencies.

For treatments using NaCl, KCl and $MnCl_2$, the best solar energy conversion efficiencies were all $<6.7\%$ owing to the low open circuit voltages and fill factor values that were associated with pronounced forward bias current limitation or 'roll-over'. These efficiencies were less than half of that of the $CdCl_2$ control and $MgCl_2$ treatments.

It is often the case that at high forward bias the current in J–V curves for CdTe cells is depressed by the presence of a non-ohmic contact; this is usually referred to as 'roll-over'[11]. This occurs due to the very high electron affinity of CdTe, meaning that a metal contact to p-type CdTe always forms a Schottky barrier. This 'roll-over' can be seen to some extent for all samples measured, but was extremely pronounced in the NaCl-, KCl- and $MnCl_2$-treated samples. Some additional 'roll-over' is also visible for $MgCl_2$ treatment in comparison to $CdCl_2$ treatment. It has been suggested that the inclusion of a $Cd_{1-x}Mg_xTe$ layer at the CdTe surface may improve the back-contact ohmicity[12]. However, in the present samples, our analyses did not indicate the presence of any $Cd_{1-x}Mg_xTe$ formation after $MgCl_2$ treatment and 'roll-over' was indeed present. In this case we attribute its presence to the formation of oxychloride surface phases similar to those which have been observed following $CdCl_2$ treatment[13] and which increase contact resistance. Measurement of the back-contact barrier height, through J–V as a function of temperature[14] (J–V–T), shows that the barrier height ϕ_b is slightly increased from 0.28 eV for $CdCl_2$ to 0.32 eV for $MgCl_2$ vapour treatment (Extended Data Fig. 1). However, through addition of a 2-nm-thick Cu layer to the back contact the barrier can be reduced to 0.23 eV, which is not anticipated to hinder device performance greatly[11,15].

The longer-term stability of $MgCl_2$-treated devices compared to $CdCl_2$-treated devices was also compared by J–V measurement both immediately after deposition and after a 6-month interval (Extended Data Fig. 2). Both devices were found to degrade identically (losing about 5% of their relative initial efficiency), consistent with the known degradation of the gold contacts used in laboratory-scale devices (that is, by oxidation of the underlying CdTe). No additional performance degradation related to $MgCl_2$ treatment was observed.

The EQE curve shapes show very little difference between the $CdCl_2$ and $MgCl_2$ treatments (Fig. 1b), indicating that the devices operate

Table 2 | Average solar-cell performance for $CdCl_2$- and $MgCl_2$-treated solar cells

Treatment	Average efficiency (%)	Average fill factor (%)	Average J_{sc} (mA cm^{-2})	Average V_{oc} (V)
$CdCl_2$	12.97 ± 0.06	70.39 ± 0.78	22.14 ± 0.16	0.827 ± 0.009
$MgCl_2$ solution	12.23 ± 0.42	69.10 ± 0.04	21.58 ± 0.73	0.820 ± 0.001
$MgCl_2$ vapour	13.03 ± 0.67	71.20 ± 1.35	22.50 ± 1.07	0.818 ± 0.011

Average solar-cell performance parameters for $MgCl_2$ vapour-treated, $MgCl_2$ solution-treated and $CdCl_2$-treated devices. Results for the $MgCl_2$ vapour and $CdCl_2$ treatments agree within bounds of error. Average and standard deviation values are from batches of nine identical solar cells.

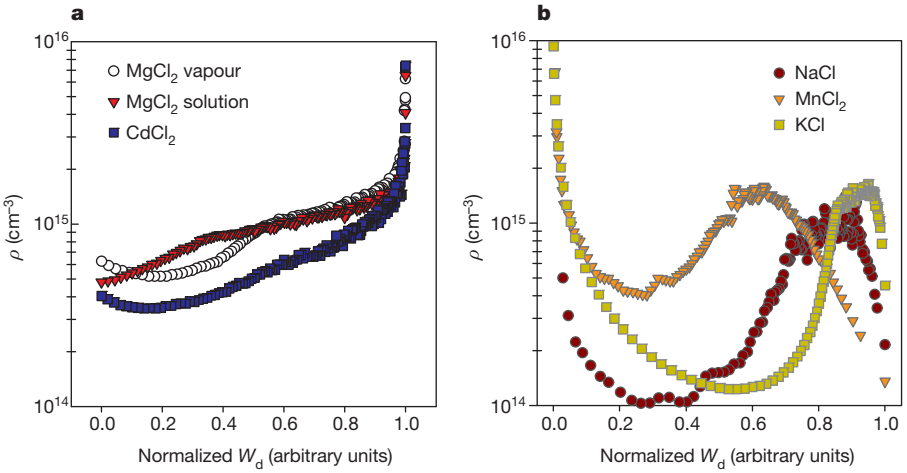

Figure 2 | Capacitance voltage profiling of carrier concentration. Hole density ρ versus normalized depletion width $W_d = \varepsilon\varepsilon_0 A/C$, determined from C–V measurements. The CdTe/CdS interface corresponds to $W_d = 0$ and $W_d = 1$ corresponds to the near-back surface point at which back-contact capacitance dominates ($V_{bias} = 500$ mV). **a**, Curves for optimized $MgCl_2$ and $CdCl_2$ treatments. The carrier density is consistently high throughout the CdTe layer, increasing towards the back contact. **b**, Curves for ineffective treatments (NaCl, $MnCl_2$ and KCl), for which the carrier concentration has a peak in the CdTe bulk, low doping at the back.

identically and that there are no major differences in the junction position or recombination behaviour. On the other hand, the ineffective chlorides NaCl, KCl and $MnCl_2$ showed different behaviour (Fig. 1d), in which the EQE decreases from short to long wavelengths. This indicates either a decreased carrier lifetime or an increase in uncompensated impurities in these devices[16] compared to $CdCl_2$ and $MgCl_2$ treatments.

Carrier density–depth profiles obtained from capacitance–voltage (C–V) data[17] are shown in Fig. 2 for all devices. Here, the apparent hole density ρ is plotted as a function of the normalized depletion width W_d, calculated from the p–n junction capacitance $W_d = \varepsilon\varepsilon_0 A/C$, with A being the contact area, C the measured capacitance, ε the relative CdTe permittivity and ε_0 the permittivity of free space. $W_d = 0$ represents the position of the CdTe/CdS interface and $W_d = 1$ is the point at which the back-contact capacitance begins to dominate ($V_{bias} > 500$ mV).

It was found that the carrier density measured in the bulk of the films that was achieved with $MgCl_2$ is comparable to or greater than the bulk carrier density in films made using $CdCl_2$, the former giving 9×10^{14} cm^{-3} and the latter 5×10^{14} cm^{-3}. Moreover, both $MgCl_2$-treated and $CdCl_2$-treated cells (Fig. 2a) show an increase in doping density towards the right-hand side of the plot, indicative of higher p doping at the back surface[17]. This increase is beneficial to device performance because it will act to reduce the extent of the Schottky behaviour. A minor feature common to both treatments is a slight increase in carrier concentration near to the front contact that may be attributed to deep levels[18].

For the ineffective treatments (Fig. 2b), the overall carrier concentrations are lower (less than 5×10^{14} cm^{-3}), and their profile shapes are noticeably different. They show peaks in carrier concentration in the bulk of the film, and a reduction towards the back contact that will act to increase its Schottky barrier width and hence contribute to the performance loss from 'roll-over'. The sharp increase in apparent doping at the near CdTe/CdS interface is an artefact of this Schottky contact: under high forward bias the contact junction undergoes a collapse, causing a decrease in capacitance that the plot interprets as a specious increase in carrier concentration[19].

Secondary ion mass spectrometry (SIMS) analysis, shown in Fig. 3, was performed on $MgCl_2$ and $CdCl_2$ samples to measure the in-diffusion of Cl and O from the post-growth treatments, this being relevant since both are linked to p-type doping in CdTe[17,20]. Indeed, the distribution of Cl and O in the depth profiles are qualitatively similar in shape to the carrier concentration profiles shown in Fig. 2 for both the $MgCl_2$-treated

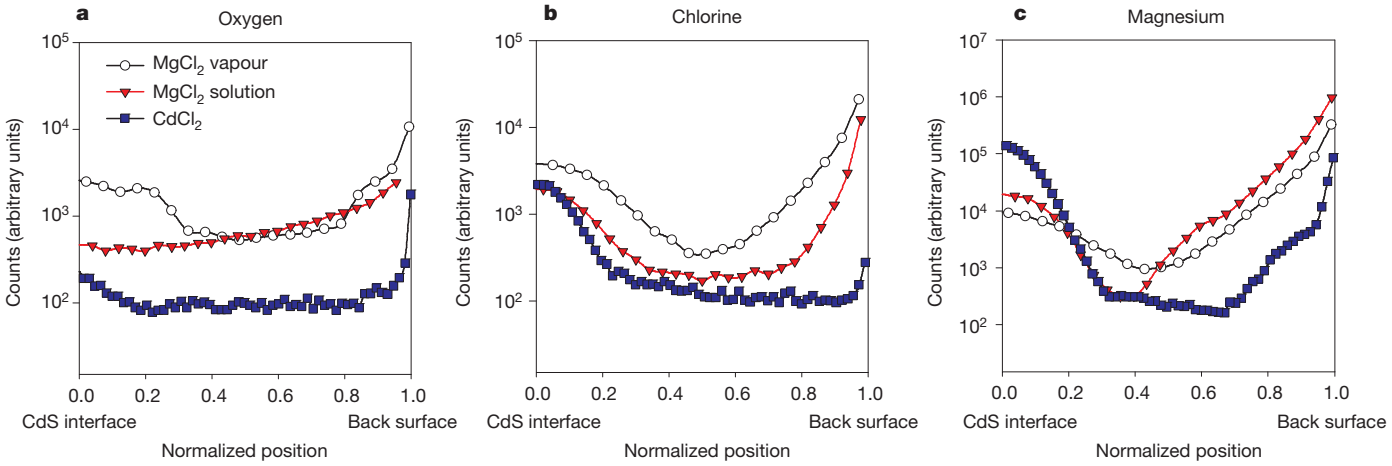

Figure 3 | SIMS profiles of CdTe films. SIMS profiles for oxygen (**a**), chlorine (**b**) and magnesium (**c**) content in $CdCl_2$-treated, $MgCl_2$-solution-treated and $MgCl_2$-vapour-treated CdTe layers. Plots have been normalized for position, so that the CdTe/CdS interface corresponds to 0 while the device back surface corresponds to 1. Analysis shows an increase in both chlorine and oxygen content in CdTe for $MgCl_2$ treatment compared to $CdCl_2$ treatment. The Mg depth profiles show that both the $CdCl_2$- and the $MgCl_2$-treated samples contain similar levels of Mg. We attribute this to out-diffusion of Mg from the soda-lime glass substrate, which contains MgO as an ingredient.

and $CdCl_2$-treated samples. However, it is also noticeable that the $MgCl_2$ treatments result in a large increase in both the Cl and O content of the CdTe layers compared to $CdCl_2$ treatment. It is likely that this is the cause of the higher p-type doping measured for $MgCl_2$ treatments.

The SIMS depth profiles for Mg in Fig. 3 show the surprising result that the levels for both the $CdCl_2$ (having no intentionally introduced Mg) and the $MgCl_2$-treated devices were comparable. This arises due to Mg out-diffusion from the soda lime glass substrate, which is known to contain about 4% MgO. Contrary to expectation, $MgCl_2$ therefore introduces no new foreign impurities to the solar cells, when compared to existing practice. It is likely that $MgCl_2$ and $CdCl_2$ have comparable doping performance on account of the electrical similarity of their doubly charged cations. On the other hand, both the singly charged ions of Na and K, and the multiple oxidation states of Mn may be expected to be electrically active centres. Their use yields altered CdTe doping profiles (Fig. 3b) and this limits the device performance.

Further to the comparative cell data provided here, improved cell performance for $MgCl_2$ activation has been achieved through a series of cell and process developments. The ZnO buffer layer was replaced with a CdS:O nanostructured film[21] and the CdS layer thickness reduced to about 40 nm. A 1 M $MgCl_2$ solution in water deposited via spray coating was used for treatment and a 2-nm Cu layer was added to improve the device back contact. This yielded a device of 15.7% efficiency (Extended Data Fig. 3), notably with a V_{oc} of 0.857 V, equivalent to that of the current CdTe champion cell[1]. This clearly demonstrates that $MgCl_2$ is capable of producing high-efficiency devices.

These results demonstrate that $MgCl_2$ may be used as a direct replacement for $CdCl_2$ in the established activation process and as such is capable of instantly reducing the cost of CdTe solar-cell production. It also eliminates the need to use any water-soluble cadmium salt. It gives carrier concentrations and doping profiles that are desirable for high-efficiency devices and its effectiveness stems from the Mg^{2+} cation being electrically inactive in CdTe, unlike other low-cost chlorides investigated. A number of factors, such as longer-term module stability testing[22], will still need to be assessed before industrial implementation. However, $MgCl_2$ processing has immense promise and has proved effective regardless of the manner in which it is applied. It is therefore likely to be robust to use under the conditions applicable for industrial application.

METHODS SUMMARY

Cell deposition. Cells were deposited on 'TEC10' soda lime glass coated with SnO_2:F supplied by NSG. 100-nm-thick ZnO buffer layers and a 120-nm-thick CdS layer were deposited by sputtering at room temperature and 200 °C respectively. CdTe layers were deposited by close space sublimation under 25 torr ambient nitrogen with source and substrate temperatures of 605 °C and 520 °C respectively. Prior to chloride treatment, cells were etched for 30 s in a nitric-phosphoric acid etch solution, followed by rinsing in deionized water. A second 30-s nitric-phosphoric etching step was applied following chloride treatment. Arrays of nine evaporated gold back-contacts (0.25 cm^2) were then applied.

Treatment methods. Three main chloride process variations were compared: (1) the 'standard' $CdCl_2$ treatment, in which a 100-nm layer was evaporated onto the CdTe surface; (2) deposition of a 10% $MgCl_2$:90% methanol solution applied to the CdTe back surface; and (3) a 10% $MgCl_2$:90% methanol solution applied to a glass slide placed in the tube furnace alongside the sample. Tests for other chloride treatments using NaCl, KCl and $MnCl_2$ were performed via a 10% chloride:90% methanol solution applied to the CdTe surface. Annealing of samples was conducted in a tube furnace in air, with temperature and times being optimized in the range 390–450 °C and 10–60 min. Optimal treatment times were 20 min at 430 °C for $MgCl_2$ solution and $CdCl_2$ treatments, and 40 min at 430 °C for $MgCl_2$ vapour treatment.

Characterization. *J–V* analysis was performed under an AM1.5 spectrum at 1,000 W m^{-2} using a TS Space Systems solar simulator. *C–V* measurements were performed in the dark using a Solatron SI1260 impedance analyser. EQE measurements were made using a Bentham PVE300 system. SIMS analysis was carried out by Loughborough Surface Analysis using a Cameca ims 4f instrument.

Online Content Methods, along with any additional Extended Data display items and Source Data, are available in the online version of the paper; references unique to these sections appear only in the online paper.

Received 26 February; accepted 28 April 2014.
Published online 25 June 2014.

1. Green, M. A., Emery, K., Hishikawa, Y., Warta, W. & Dunlop, E. D. Solar cell efficiency tables (version 43). *Prog. Photovolt. Res. Appl.* **22,** 1–9 (2014).
2. Zweibel, K. The impact of tellurium supply on cadmium telluride photovoltaics. *Science* **328,** 699–701 (2010).
3. McCandless, B. E., Moulton, L. V. & Birkmire, R. W. Recrystallization and sulfur diffusion in $CdCl_2$-treated CdTe/CdS thin films. *Prog. Photovolt. Res. Appl.* **5,** 249–260 (1997).
4. Moutinho, H. R. *et al.* Studies of recrystallization of CdTe thin films after $CdCl_2$ treatment. In *Conference Record of the Twenty Sixth IEEE Photovoltaic Specialists Conference (Anaheim, California)* 431–434 (IEEE, 1997).
5. Edwards, P. R., Galloway, S. A. & Durose, K. EBIC and luminescence mapping of CdTe/CdS solar cells. *Thin Solid Films* **372,** 284–291 (2000).
6. Basol, B. M., Ou, S. S. & Stafsudd, O. M. Type conversion, contacts, and surface effects in electroplated CdTe-films. *J. Appl. Phys.* **58,** 3809–3813 (1985).
7. Fthenakis, V. M. & Kim, H. C. CdTe photovoltaics: life cycle environmental profile and comparisons. *Thin Solid Films* **515,** 5961–5963 (2007).
8. Mazzamuto, S. *et al.* A study of the CdTe treatment with a freon gas such as CHF_2Cl. *Thin Solid Films* **516,** 7079–7083 (2008).
9. Balarew, C. Solubilities in seawater-type systems—some technical and environmental friendly applications. *Pure Appl. Chem.* **65,** 213–218 (1993).
10. Liu, Z. S. & Chang, S. K. C. Optimal coagulant concentration, soymilk and tofu quality as affected by a short-term model storage of proto soybeans. *J. Food Process. Preserv.* **32,** 39–59 (2008).
11. Demtsu, S. H. & Sites, J. R. Effect of back-contact barrier on thin-film CdTe solar cells. *Thin Solid Films* **510,** 320–324 (2006).
12. Drayton, J., Geisthardt, R., Raguse, J. & Sites, J. R. Metal chloride passivation treatments for CdTe solar cells. *Mater. Res. Soc. Symp. Proc.* **1538,** 269–274 (2013).
13. Waters, D. *et al.* Surface analysis of CdTe after various pre-contact treatments. In *Proceedings of the 2nd World Conference and Exhibition of Photovoltaic Solar Energy Conversion* 1031–1034 (European Commission Joint Research Centre, 1995).
14. Bätzner, D. L., Oszan, M. E., Bonnet, D. & Bucher, K. Device analysis methods for physical cell parameters of CdTe/Cds solar cells. *Thin Solid Films* **361/362,** 288–292 (2000).
15. Fahrenbruch, A. L. Exploring back contact technology to increase CdS/CdTe solar cell efficiency. *Mater. Res. Soc. Symp. Proc.* **1012,** abstr. 1012-Y07-05 (2007).
16. Kosyachenko, L. & Toyama, T. Current-voltage characteristics and quantum efficiency spectra of efficient thin-film CdS/CdTe solar cells. *Sol. Energy Mater. Sol. Cells* **120,** 512–520 (2014).
17. Proskuryakov, Y. Y. *et al.* Doping levels, trap density of states and the performance of co-doped CdTe(As,Cl) photovoltaic devices. *Sol. Energy Mater. Sol. Cells* **93,** 1572–1581 (2009).
18. Burgelman, M., Nollet, P. & Degrave, S. Electronic behaviour of thin-film CdTe solar cells. *Appl. Phys. A* **69,** 149–153 (1999).
19. Li, J. V. *et al.* Theoretical analysis of effects of deep level, back contact, and absorber thickness on capacitance-voltage profiling of CdTe thin-film solar cells. *Sol. Energy Mater. Sol. Cells* **100,** 126–131 (2012).
20. Tyan, Y. S., Vazan, F. & Barge, S. Effect of oxygen on thin-film CdS/CdTe solar cells. In *Conference Record of the Twenty Sixth IEEE Photovoltaic Specialists Conference (Kissimmee, Florida)* 840–845 (IEEE, 1984).
21. Wu, X. *et al.* Nanostructured CdS: O film: preparation, properties, and application. In *11th International Conference on II–VI Compounds Proceedings* 1062–1066 (Wiley-VCH, 2004).
22. Barth, K. L., Enzenroth, R. A. & Sampath, W. S. Consistent processing and long term stability of CdTe devices. In *Conference Record of the Twenty First IEEE Photovoltaic Specialists Conference (Lake Buena Vista, Florida)* 323–326 (IEEE, 2005).

Acknowledgements We thank T. Veal for assistance in manuscript preparation and the Engineering and Physical Sciences Research Council for funding support.

Author Contributions J.D.M. and R.E.T. conceived the experiments. J.D.M. fabricated and tested the solar-cell devices. L.J.P. performed *C–V* measurements. J.D.M. and K.D. discussed the results and prepared the manuscript.

Author Information Reprints and permissions information is available at www.nature.com/reprints. The authors declare no competing financial interests. Readers are welcome to comment on the online version of the paper. Correspondence and requests for materials should be addressed to J.D.M. (jon.major@liverpool.ac.uk).

METHODS

Cell deposition. CdTe solar-cell devices were fabricated in the 'superstrate' configuration on commercial soda lime glass substrates (NSG TEC10 from NSG) coated with fluorine-doped tin oxide. Radio-frequency sputtering was used to deposit a 100-nm ZnO 'buffer' layer onto the fluorine-doped tin oxide by reactively sputtering from a Zn target in the presence of oxygen. A 120-nm-thick CdS layer window layer was then deposited by radio-frequency sputtering at a substrate temperature of 200 °C under ambient Ar and using a power of 60 W. CdTe absorber layers were deposited via close space sublimation deposition, using a custom all-quartz deposition chamber manufactured by Electro-Gas Systems. Deposition was carried out at source and substrate temperatures of 615 °C and 520 °C respectively, under a pressure of 30 torr of nitrogen, giving a thickness of about 4 μm. Following CdTe deposition, the samples were submerged for 15 s in a nitric-phosphoric acid etch solution. This created a Te-rich back surface to the CdTe layer and has been found to aid in-diffusion during post-growth activation[23]. Following activation treatment (described below), samples were subjected to a further 15 s nitric-phosphoric etch before the deposition of 0.25 cm^2 gold back contacts by vacuum evaporation to complete the device.

Post growth activation treatments. A number of different post-growth treatment routes were compared in this work. Following deposition of the Cl-containing layer, all samples were annealed in a tube furnace under an air ambient. For each Cl treatment the annealing time and temperature was optimized in the range 10–60 min and 390–450 °C. This was done to ensure the maximum attainable performance level achievable by each treatment was accurately established. For each treatment time and temperature a complete device was fabricated and its performance was assessed via *J*–*V* analysis. The treatment which yielded the highest device efficiencies in each case was identified. Over 150 devices were processed during the course of this optimization.

For the standard $CdCl_2$ treatment, $CdCl_2$ (99.99% purity, Sigma Aldrich product number 202908) was deposited onto the CdTe back surface as a 100-nm-thick thin film via thermal evaporation, as this is the established deposition practice for cell production. Optimum treatment conditions were a 20-min anneal at 430 °C. Treatment using alternative chlorides—NaCl, KCl and $MnCl_2$—was performed via a few drops of 10% chloride: 90% methanol solution applied to the CdTe back surface before annealing. In the case of $MgCl_2$ (99+% purity, Alfa Aesar product number 12315), two different processing routes were initially investigated: (1) the $MgCl_2$ 'solution' treatment, in which a few drops of 10% $MgCl_2$:90% methanol solution were applied directly to the CdTe back surface; and (2) the $MgCl_2$ 'vapour' treatment, in which a few drops of 10% $MgCl_2$:90% methanol solution were applied to a glass slide placed in the tube furnace alongside the CdTe sample. Optimal processing conditions were found to be 20 min at 430 °C for $MgCl_2$ solution processing and 40 min at 430 °C for $MgCl_2$ vapour processing.

Current–voltage measurement. *J*–*V* analysis was performed under an AM1.5 spectrum at 1,000 W m^{-2} using a TS Space Systems solar simulator.

External quantum efficiency measurement. EQE measurements were made using a Bentham PVE300 system.

Capacitance–voltage measurements. *C*–*V* measurements were performed in the dark using a Solatron SI1260 impedance analyser and a frequency of 10 kHz. *C*–*V* data were recalculated into depth–density profiles using the method detailed in Blood and Orton[24]. Only data recorded for bias <0.5 V were used, as at high forward bias the device back contact may dominate the capacitance response[17].

SIMS. SIMS analysis was carried out by Loughborough Surface Analysis using a Cameca ims 4f instrument.

Back contact barrier height measurement. The formation of ohmic contacts to p-type CdTe is difficult owing to the high electron affinity of CdTe ($\chi_s = 4.5$ eV), meaning that a metal of work function >6.0 eV is required. Most metal contacts to CdTe therefore form a Schottky barrier at the back contact and this leads to the phenomenon of 'roll-over' (that is, a decrease in rate of current increase) at high forward bias. The back-contact barrier height may be determined from dark *J*–*V* measurements as a function of temperature: *J*–*V*–*T* measurement. Using the method proposed by Bätzner *et al.*[14], the series resistance, R_s, is determined at forward bias above V_{oc} as a function of temperature. $R_s(T)$ may then be separated into an ohmic and and exponential component, which results from passage of the carriers over the back contact via thermionic emission. R_s may be expressed as follows:

$$R_s = R_{\Omega_0} + \frac{\partial R_{\Omega_0}}{\partial T} T + \frac{C}{T^2} e^{\left(\frac{b}{kT}\right)}$$

where R_{Ω_0} and $\frac{\partial R_{\Omega_0}}{\partial T}$ are the ohmic resistance and its temperature coefficient respectively. K is the Boltzmann constant and C is a fitting parameter. The barrier height ϕ_b may therefore be determined via exponential fitting of $R_s(T)$. *J*–*V*–*T* measurements were performed in a cryostat (CTI Cryogenics) using a temperature range of 150–350 K.

$CdTe_{1-x}Mg_x$ as a potential electron back reflector. There has been no evidence reported to suggest Mg may act as an electrically active impurity centre in CdTe. The most likely form Mg may be expected to take in CdTe is via the formation of $CdTe_{1-x}Mg_x$ alloyed phases. Rather than being problematic, $CdTe_{1-x}Mg_x$ has in fact been investigated as a candidate for an electron back reflector layer for CdTe[25], owing to its excellent lattice matching to CdTe and expanded bandgap. The electron back reflector concept involves the incorporation of a wider bandgap material with a negligible valence band offset between the CdTe and back contact, thus forming a potential barrier in the device conduction band. This barrier reflects minority carrier electrons away from the back surface, thus reducing the back-surface recombination and improving the V_{oc} (ref. 26). As we have shown in this work, Mg may indeed be diffused into the CdTe without unduly comprising the CdTe doping profile and device performance, so $CdTe_{1-x}Mg_x$ does have significant potential as an electron reflector layer. However, while it seems probable that some $CdTe_{1-x}Mg_x$ phases may be present, as yet we are unable to find evidence of alloyed $CdTe_{1-x}Mg_x$ layers being formed during $MgCl_2$ processing.

Additional $MgCl_2$ process development. Following the self-consistent comparative study of different Cl treatments, alterations to the cell structure and processing were made to improve the peak device performance attainable (see Extended Data Fig. 3). These changes to the cell fabrication process are listed below.

CdS:O nanostructured window layer. Nanostructured CdS:O window layers, which have an increased bandgap owing to quantum confinement effects[21], were incorporated to replace the SnO_2/CdS buffer and window layer stack. Deposition was performed by radio-frequency sputtering using 60 W of power and at room temperature. A mixed argon/oxygen ambient gas was used with a 7% oxygen composition, giving a film with an as-deposited bandgap of about 3.9 eV and a film thickness of 250 nm. During CdTe deposition a portion of the CdS:O layer recrystallizes to form a thin (~40 nm) CdS layer, with a bandgap of 2.4 eV as the CdTe interface.

Aqueous $MgCl_2$ solution processing. Further development of the $MgCl_2$ post-growth treatment has led to $MgCl_2$ being deposited from a 1 M solution in deionized water. The $MgCl_2/H_2O$ solution is spray deposited onto the back surface of the CdTe before annealing, allowing much finer control and uniformity. In addition, this negates any issues regarding the hygroscopic nature of $MgCl_2$. Optimal processing conditions were found to be 20 min annealing at 430 °C in air. This is now established as the preferred route for $MgCl_2$ deposition, as it requires the use of no solvents or thermal deposition equipment and has led to improved device efficiencies.

Cu back-contacting. Cu back-contacting is known to reduce the back-contact barrier in CdTe devices via the formation of a Cu_xTe_{1-x} phase at the CdTe free surface. Following post-growth activation treatment the cell is etched in nitric-phosphoric solution to form a Te-rich surface. A 2-nm-thick Cu film is then deposited via thermal evaporation before annealing at 150 °C for 20 min under vacuum. The back contact is then completed by the deposition of 60-nm of Au via thermal evaporation at room temperature.

23. Major, J. D., Proskuryakov, Y. Y. & Durose, K. Impact of CdTe surface composition on doping and device performance in close space sublimation deposited CdTe solar cells. *Prog. Photovolt. Res. Appl.* **21,** 436–443 (2013).
24. Blood, P. & Orton, J. *The Electrical Characterisation of Semiconductors: Majority Carriers and Electron States* 220–264 (Academic, 1992).
25. Kobyakov, P. S., Geisthardt, R., Cote, T. & Sampath, W. S. Growth and characterization of $Cd_{1-x}Mg_xTe$ thin films for possible application in high-efficiency solar cells. In *Conference Record of the Twenty Sixth IEEE Photovoltaic Specialists Conference (Austin, Texas)* 160–163 (IEEE, 2012).
26. Hsiao. K-J. & Sites, J. R. Electron reflector to enhance photovoltaic efficiency: application to thin-film CdTe solar cells. *Prog. Photovolt. Res. Appl.* **20,** 486–489 (2012).

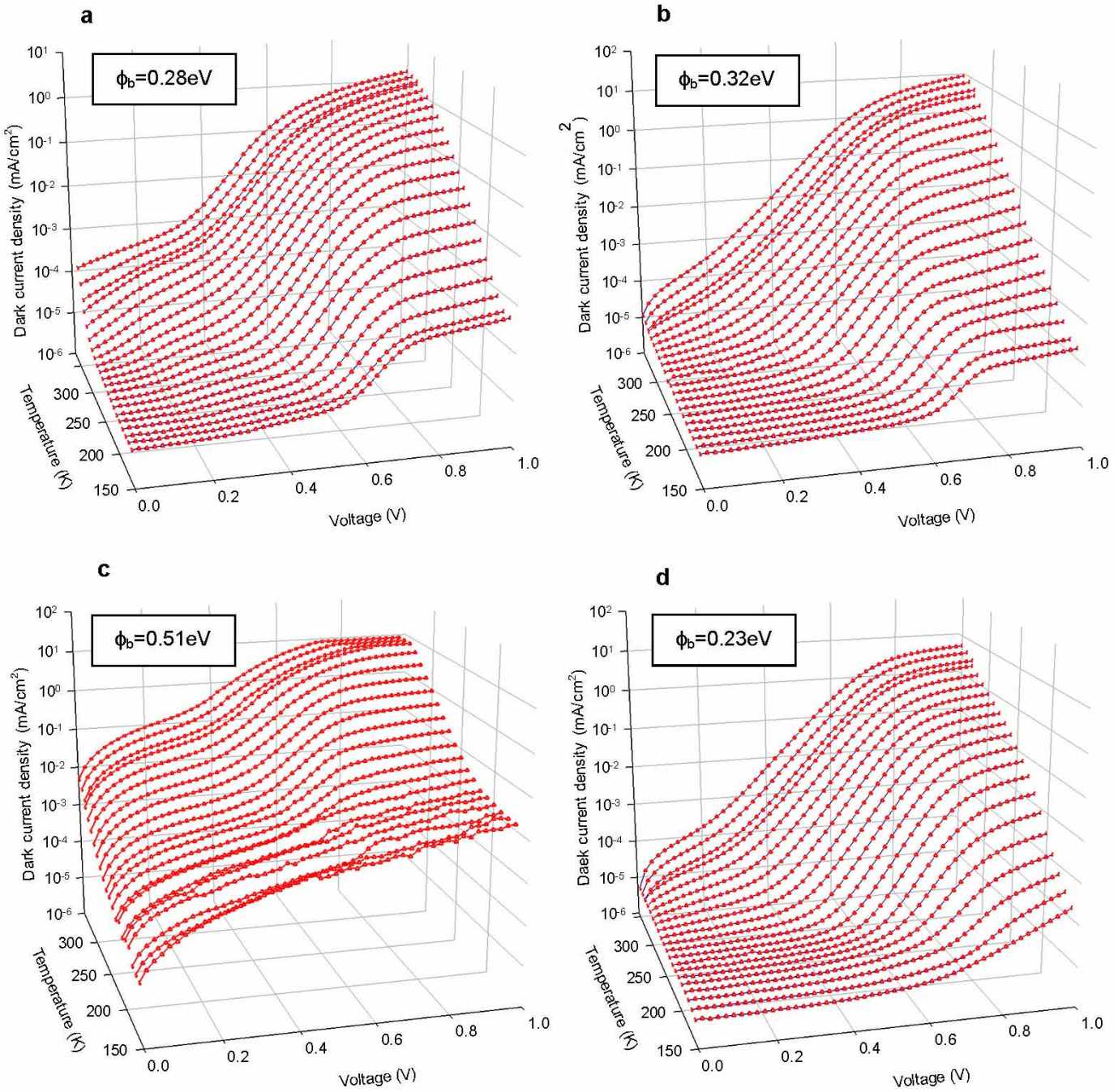

Extended Data Figure 1 | *J–V–T* data for cells with various chloride treatments. Current density versus voltage curves measured as a function of temperature (*J–V–T*) with inset back-contact barrier height values ϕ_b, determined for the highest-efficiency contacts for: the $CdCl_2$-treated device (**a**), the $MgCl_2$-vapour-treated device (**b**), the NaCl-treated device (**c**) and the high-efficiency cell (see Extended Data Fig. 3) treated with a 1 M $MgCl_2/H_2O$ solution and addition of 2 nm Cu to the back contact (**d**). Values for the back-contact barrier height are extracted by fitting to the temperature dependence of the series resistance R_s (see Methods).

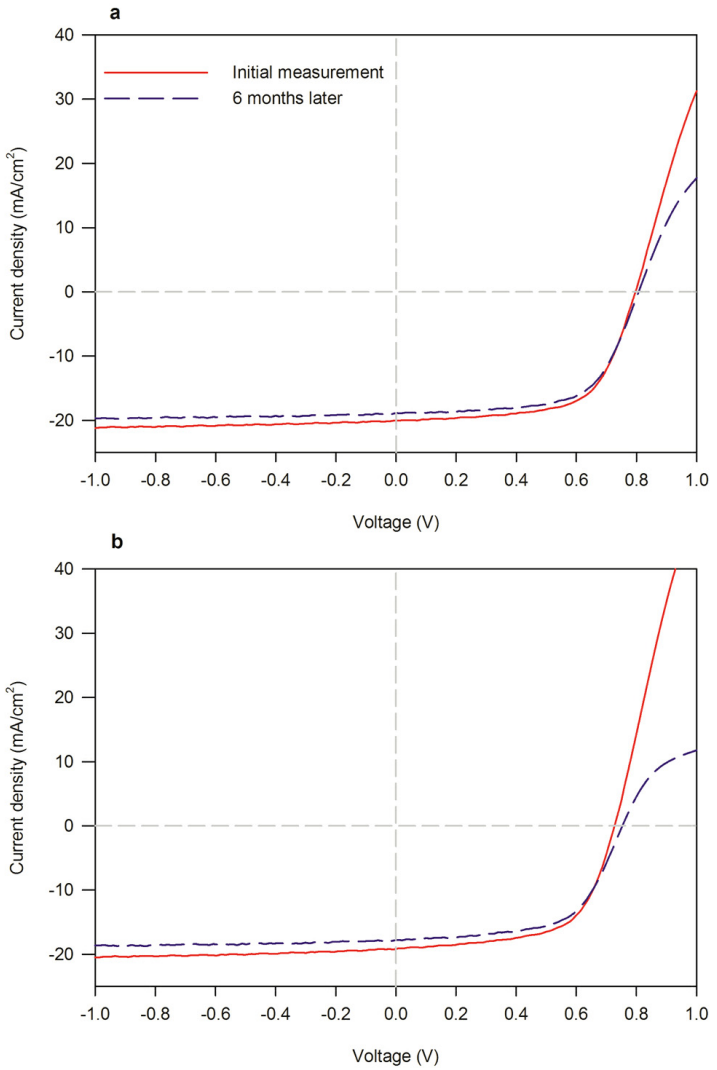

c

	Average performance ratio	Error
Efficiency	0.949	±0.032
Fill factor	0.997	±0.028
J_{SC}	0.945	±0.005
V_{OC}	1.008	±0.012

d

	Average performance ratio	Error
Efficiency	0.943	±0.011
Fill factor	0.987	±0.005
J_{SC}	0.929	±0.009
V_{OC}	0.987	±0.006

Extended Data Figure 2 | Stability measurements for $CdCl_2$- and $MgCl_2$-treated cells. *J–V* curves for devices treated with the $MgCl_2$ vapour process (**a**) and the $CdCl_2$ treatment (**b**). *J–V* curves were measured immediately after processing and then after 6 months of storage under ambient conditions. Performance degradation over the 6-month period was assessed from the average shift in efficiency, fill factor, short circuit current density J_{sc} and open circuit voltage V_{oc} for nine contacts over this period. The averages for the ratio of initial and final performances, along with the associated error, are given for the $MgCl_2$ vapour treatment (**c**) and the $CdCl_2$ treatment (**d**).

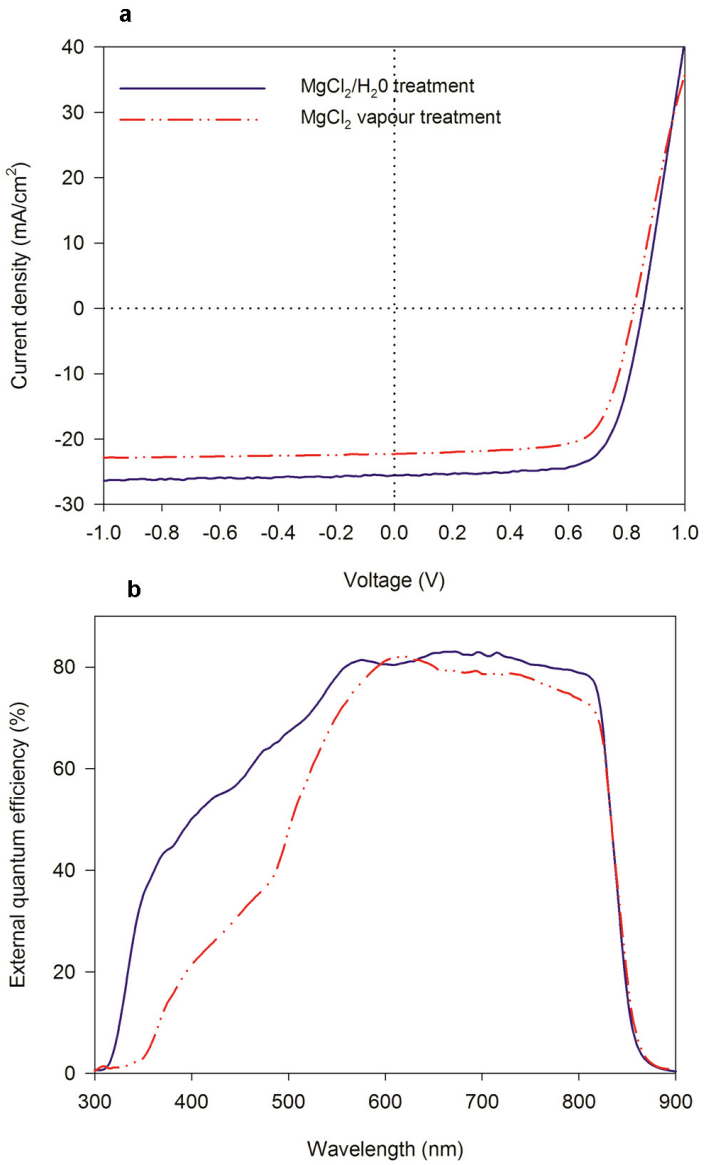

c

Treatment	Efficiency (%)	Fill factor (%)	J_{SC} (mA/cm^2)	V_{OC} (V)
$MgCl_2/H_2O$	15.7	71.29	25.54	0.857
$MgCl_2$ Vapour	13.5	70.24	23.26	0.826

Extended Data Figure 3 | High-efficiency $MgCl_2$-treated devices. Performance of CdTe devices treated with $MgCl_2$ is further improved following device optimization and the use of a 1 M $MgCl_2/H_2O$ solution. A 2-nm Cu layer is added to the back contact, the ZnO buffer layer is replaced with a nanostructured CdS:O layer and CdS thickness is reduced to about 40 nm. **a**, *J*–*V* curves for the unimproved $MgCl_2$-vapour-treated device (13.5%), and the improved cell treated with $MgCl_2/H_2O$ solution (15.7%). **b**, EQE curves for the same devices, showing minimised CdS/ZnO cut-off at short wavelength (300–525 nm) by use of CdS:O layer. **c**, Extracted device performance parameters from *J*–*V* data.